Available online at www.sciencedirect.com
ScienceDirect
Optical Materials 30 (2008) 1213–1216
OPTICAL Materials
www.elsevier.com/locate/optmat

Spatiotemporal instabilities of counterpropagating beams in nematic liquid crystals

A.I. Strinić [a,*], D.M. Jović [a], M.S. Petrović [a], D.V. Timotijević [a], N.B. Aleksić [a], M.R. Belić [b]

[a] *Institute of Physics, Pregrevica 118, 11080 Belgrade, Zemun, Serbia*
[b] *Texas A&M University at Qatar, P.O. Box 5825, Doha, Qatar*

Available online 13 July 2007

Abstract

We investigate the behavior of counterpropagating self-trapped optical beam structures in nematic liquid crystals. We treat numerically a time-dependent model for the beam propagation and the director reorientation in a nematic liquid crystal, in $(2+1)$ spatial dimensions. The formation of stable solitons in a narrow threshold region of control parameters is displayed. Spatiotemporal instabilities are observed as the input intensity, the propagation distance, and the birefringence are increased. Transverse displacement, filamentation, and dynamical instabilities of counterpropagating beams are demonstrated.

PACS: 42.65.Sf; 42.65.Tg; 42.70.Df

Keywords: Nematic liquid crystals; Optical counterpropagating beams; Dynamical behavior

1. Introduction

Nematic liquid crystals (NLC) are known to exhibit enormous optical nonlinearities, owing to large refractive index anisotropy, coupled with the optically-induced collective molecular reorientation. They behave in a fluid-like fashion, but display long-range order that is characteristic of crystals [1]. Thanks to nonlinear, saturable, nonlocal and nonresonant response, the propagation of self-focused beams [2] in NLC has been the subject of considerable interest in recent years, from both experimental [3,4] and theoretical points of view [5–7]. However, most of the accounts deal with the propagation in one direction. The only study of counterpropagating (CP) beams in NLC that we are aware of, was reported in [8], and it deals with an experimental observation of waveguiding due to nonlocal thermal nonlinearity.

We investigate the behavior of CP self-focused beams, both in time and in three spatial dimensions, using an appropriately developed theoretical model and a numerical procedure based on the beam propagation method. We find that solitons exist in a narrow region of beam intensities, and at lower values than in the case of copropagating beams [5]. Below this region the beams diffract, above the beams display dynamical and even chaotic behavior. A new feature here is that for higher intensities a transversal motion of beams (transverse undulating displacement) is observed. We also consider the propagation of broader CP Gaussian beams, which offers opportunities for observing a complex pattern-forming dynamical behavior. The propagation and interactions of more complicated beam structures, such as optical vortices, are also studied.

2. The model

The unique property of NLC is their ability to change optical properties under the action of an external electric field, which enables the macroscopic reorientation of the director θ of NLC. The evolution of slowly-varying beam envelopes A and B, linearly polarized along x axis and

* Corresponding author. Tel.: +381 11 3160260; fax: +381 11 3162190.
E-mail address: strinic@phy.bg.ac.yu (A.I. Strinić).

0925-3467/$ - see front matter © 2007 Elsevier B.V. All rights reserved.
doi:10.1016/j.optmat.2007.05.053

propagating along z axis, is well described by the following paraxial wave equations [9]:

$$2ik\frac{\partial A}{\partial z} + \Delta_{x,y}A + k_0^2\varepsilon_a(\sin^2\theta - \sin^2(\theta_{rest}))A = 0, \quad (1)$$

$$-2ik\frac{\partial B}{\partial z} + \Delta_{x,y}B + k_0^2\varepsilon_a(\sin^2\theta - \sin^2(\theta_{rest}))B = 0, \quad (2)$$

where A and B are the forward and backward propagating beam envelopes, $k = k_0 n_0$ is the wave vector in the medium and $\varepsilon_a = n_e^2 - n_0^2$ is the birefringence of the medium. The rest distribution angle θ_{rest} in the presence of a low-frequency electric field is modeled by [9]

$$\theta_{rest}(z,V) = \theta_0(V) + [\theta_{in} - \theta_0(V)] \cdot \left[\exp(-z/\bar{z}) + \exp-\frac{(L-z)}{\bar{z}}\right], \quad (3)$$

with $\theta_0(V)$ being the orientation distribution due to the applied voltage far from the input interface. θ_{in} is the director orientation at the boundaries $z = 0$ and $z = L$, where L is the propagation distance and $\bar{z}$ is the relaxation distance. The temporal evolution of the angle of reorientation is given by the diffusion equation [1,7]

$$\gamma\frac{\partial\theta}{\partial t} = K\Delta_{x,y}\theta + \frac{1}{4}\varepsilon_0\varepsilon_a\sin(2\theta)\left\{|A|^2 + |B|^2\right\}, \quad (4)$$

where γ is the viscous coefficient and K is Frank's elastic constant. Here θ is the overall tilt angle, owing to both the light and the voltage influence. Using the rescaling $z = zkx_0^2$, $x = xx_0$, $y = yx_0$, and $t = t\tau$, we transform the equations into a dimensionless form:

$$2i\frac{\partial A}{\partial z} + \Delta_{x,y}A + k_0^2x_0^2\varepsilon_a(\sin^2\theta - \sin^2(\theta_{rest}))A = 0, \quad (5)$$

$$-2i\frac{\partial B}{\partial z} + \Delta_{x,y}B + k_0^2x_0^2\varepsilon_a(\sin^2\theta - \sin^2(\theta_{rest}))B = 0, \quad (6)$$

$$\frac{\partial\theta}{\partial t} = \frac{K\tau}{\gamma x_0^2}\Delta_{x,y}\theta + \frac{\varepsilon_0\varepsilon_a\tau}{4\gamma}\sin(2\theta)\left\{|A|^2 + |B|^2\right\}, \quad (7)$$

where τ is the relaxation time and x_0 is the transverse scaling length. Eqs. (5)–(7) form the basis of our model. By solving these equations we will be describing the propagation of beams in both space and time. We develop a novel numerical procedure, based on FFT, utilizing our prior experience in treating beam propagation in nematic liquid crystals [5].

3. Results and discussion

Numerical studies of partial differential equations describing the beam propagation in electrically biased plane-oriented NLC are performed in different conditions and for a variety of beam configurations. The propagation of CP narrow and broad Gaussian beams, as well as of CP vortices is investigated. All the pictures in the transverse (x,y) plane are presented at the exit face of the crystal $(z = L)$, and all the pictures in the (y,z) plane are at the $x = 0$ plane (in the middle of the crystal). All the pictures are presented for one beam (the forward) only. In all figures the times are indicated, except when the steady-state is reached.

In all the simulations the following data are kept constant: the diffraction length $Ld = kx_0^2 = 79$ μm, the propagation distance $L = 6.3Ld = 0.5$ mm, the transverse scaling length $x_0 = 2$ μm, the laser wavelength $\lambda = 514$ nm, the relaxation distance $\bar{z} = 40$ μm, the elastic constant $K = 0.7\times10^{-11}$ N, the viscous coefficient $\gamma = 0.08$ kg/ms, the ordinary refractive index $n_0 = 1.53$, the director orientation at the boundary $\theta_{in} = \pi/2$, the orientation distribution $\theta_0 = \pi/4$, the birefringence $\varepsilon_a = 0.5$. All of these data are consistent with the values reported in the experimental investigations [10,11].

First we consider the behavior of CP Gaussian beams in NLC, by increasing the beam intensity. The effect of the input intensity variation on the CP Gaussian beam propagation is presented in Fig. 1. For smaller intensities (Fig. 1a) self-focusing is too weak to keep the beam tightly focused, so it can not pass through unchanged, as a spatial soliton. By increasing the beam intensity (Fig. 1b) at one point stable solitonic propagation is achieved. For still higher intensities we observe transversal motion of the beam, in the form of one (Fig. 1c), or two consecutive (Fig. 2) jumps, resembling beam undulations. For further increase of the intensity we see unstable dynamical behavior of beams (Fig. 1d).

The displayed displacements in CP geometry have no counterparts in the copropagating (CO) geometry [5]. For narrow CP beams (4 μm) the intensity needed for soliton existence (to pass through the medium without diffraction) is about three times lower than in the CO case [5]. The same conclusion holds for the broader beams, with input FWHM = 20 μm (Fig. 3). In Fig. 3, we compare the behavior of CO and CP cases. As expected, similar behavior is seen, but it occurs at different input beam intensities. By increasing the beam intensity (the first row) we achieve stable propagation, i.e., solitonic propagation in both cases. At higher intensities we observe different kinds of instabil-

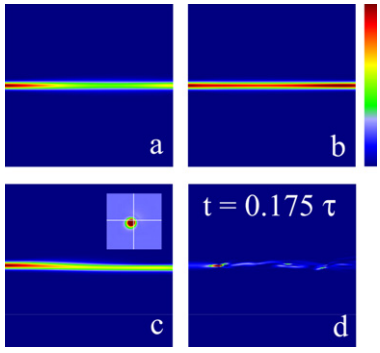

Fig. 1. Beam propagation, shown for one beam in the (y,z) plane, for different input intensities: (a) $I = 6\times10^{+9}$ V^2/m^2, (b) $I = 7\times10^{+9}$ V^2/m^2, (c) $I = 8\times10^{+9}$ V^2/m^2, and (d) $I = 9\times10^{+10}$ V^2/m^2. In (c) the beam intensity is also shown in the (x,y) plane. For all simulations FWHM = 4 μm, $L = 0.5$ mm, and $\varepsilon_a = 0.5$.

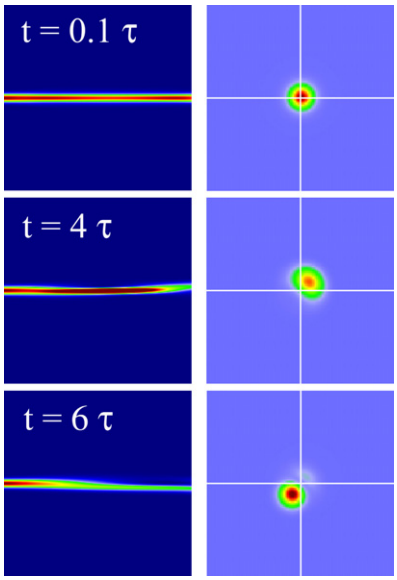

Fig. 2. Beam propagation, shown for one beam in the (y,z) plane (the first column) and in the (x,y) plane (the second column), at different times. Parameters: $I = 1\times10^{+10}\,\mathrm{V^2/m^2}$, FWHM = 4 μm, $L = 0.5$ mm, and $\varepsilon_a = 0.5$.

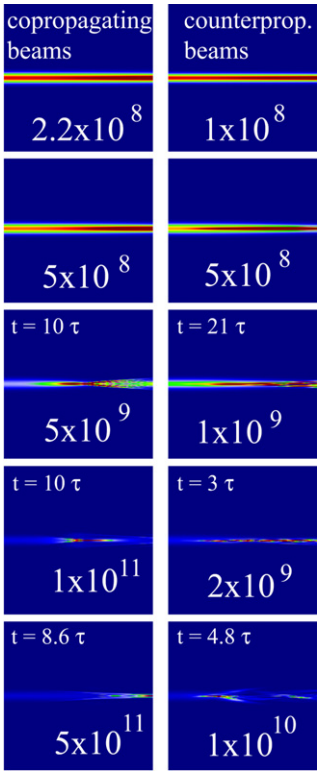

Fig. 3. Comparison between copropagating (the first column) and counterpropagating (the second column) beams in NLC, for different input intensities, indicated in the figures. For all the simulations input FWHM = 20 μm, $L = 0.5$ mm, and $\varepsilon_a = 0.5$.

ities: soliton breathing (the second row), stable filamentation (the third and fourth rows), and dynamical instabilities (the fifth row).

Next we consider the behavior of broader CP Gaussian beams in NLC (Fig. 4). We utilize broader Gaussian beams in numerical simulations, in order to display modulational instabilities and pattern formation of broader CP beams. For two different values of the input beam intensity we vary the input FWHM of Gaussian beams. By increasing FWHM, we get more regular patterns following an irregular dynamical behavior, unlike the case of CP broad Gaussians in photorefractive crystals [12]. There one sees ordered patterns first, which become increasingly irregular. This behavior is the consequence of the long-range order that is characteristic of NLC, in contrast to the local interaction, characteristic of the isotropic photorefractive medium. Another feature of broad CP beams in NLC is a relatively long time needed to achieve steady-state.

Besides varying beam parameters, we also vary the birefringence (ε_a), which characterizes the medium (Fig. 5). In Fig. 5, we show the propagation for $\varepsilon_a = 0.8$. One can see that for different input intensities the instabilities develop similarly to the case $\varepsilon_a = 0.5$ considered in Fig. 1. The values of intensity where the stable soliton propagation is observed are different for the two cases. For higher ε_a this

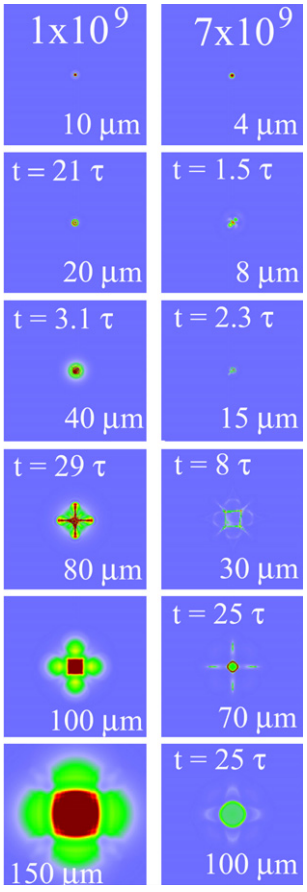

Fig. 4. Intensity distributions at the output face of the crystal for two values of intensities: $I = 1\times10^{+9}\,\mathrm{V^2/m^2}$ (the first column) and $I = 7\times10^{+9}\,\mathrm{V^2/m^2}$ (the second column), for different input FWHM of beams (indicated in each figure). In all simulations $L = 0.5$ mm and $\varepsilon_a = 0.5$.

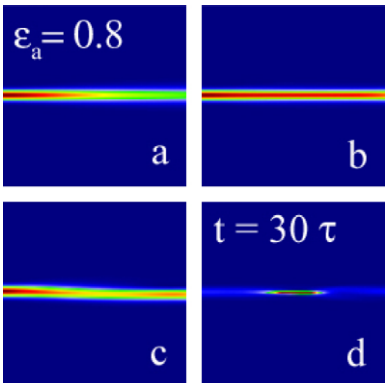

Fig. 5. Intensity distributions for $\varepsilon_a = 0.8$ and for different input intensities: (a) $I = 2 \times 10^{+9}$ V^2/m^2, (b) $I = 2.7 \times 10^{+9}$ V^2/m^2, (c) $I = 3 \times 10^{+9}$ V^2/m^2, and (d) $I = 7 \times 10^{+9}$ V^2/m^2. In all simulations FWHM = 4 μm and $L = 0.5$ mm.

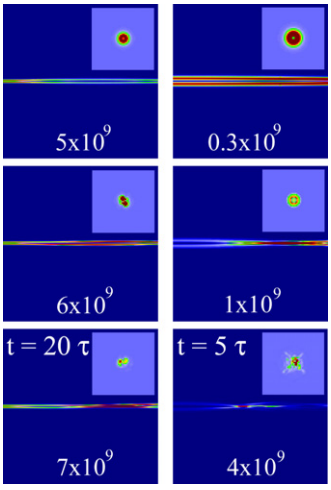

Fig. 6. CP vortices interaction for different input FWHM: 8 μm (the first column) and 23 μm (the second column), and for different intensities. The first row: stable vortex propagation. The second row: filamentation. The third row: dynamic instabilities. Insets depict transverse intensity distributions. In all simulations $L =$ 0.5 mm and $\varepsilon_a = 0.5$.

value is smaller (in the case $\varepsilon_a = 0.8$ the intensity where stable soliton appears is $2.7 \times 10^{+9}$ V^2/m^2, whereas for $\varepsilon_a = 0.5$ the soliton appears at $I = 7 \times 10^{+9}$ V^2/m^2).

Finally, we consider the interaction of CP vortices with opposite topological charges (±1) in NLC. The input beam intensities are varied for two values of the input FWHM (Fig. 6). We find stable vortex propagation for lower intensities (the first row), as well as standing waves in the form of dipoles and quadrupoles for higher intensities (the second row). By further increasing the input beam intensities, an irregular behavior is observed (the third row).

4. Conclusion

We investigated numerically the behavior of CP self-focused beam structures in NLC. We demonstrated different nontrivial and novel properties caused by the nonlocal nature of the nonlinear response of NLC. For narrow CP Gaussian beams we discover transverse motion of the beams, as well as filamentation and irregular dynamics. In the case of broader Gaussian beams, by increasing FWHM of input beams, regular patterns after an irregular dynamical behavior are displayed. For CP vortices a stable vortex propagation, standing waves and irregular behavior are observed, depending of the beam parameters.

Acknowledgements

Work at the Institute of Physics is supported by the Ministry of Science and Environmental Protection of the Republic of Serbia, under the Project OI 141031. We are thankful to the IT Center of the Texas A&M University at Qatar, for allowing us to use the SAQR supercomputing cluster.

References

[1] I.C. Khoo, Liquid Crystals: Physical Properties and Nonlinear Optical Phenomena, Wiley, New York, 1995.
[2] Y.S. Kivshar, G.P. Agrawal, Optical Solitons, Academic Press, San Diego, 2003.
[3] M. Peccianti, C. Conti, G. Assanto, J. Nonlin. Opt. Phys. Mater. 12 (2003) 525.
[4] X. Hutsebaut, C. Cambournac, M. Haelterman, J. Beeckman, K. Neyts, J. Opt. Soc. Am. B 22 (2005) 1424.
[5] A.I. Strinić, D.V. Timotijević, D. Arsenović, M.S. Petrović, M.R. Belić, Opt. Exp. 13 (2005) 493.
[6] P.D. Rasmussen, O. Bang, W. Krolikowski, Phys. Rev. E 72 (2005) 066611.
[7] G. D'Alessandro, A.A. Wheeler, Bistability of liquid crystal microcavities, Phys. Rev. A 67 (2003) 023816.
[8] J.F. Henninot, M. Debailleul, M. Warenghem, Mol. Cryst. Liq. Cryst. 375 (2002) 631.
[9] M. Peccianti, A. De Rossi, G. Assanto, A. De Luca, C. Umeton, I. Khoo, Appl. Phys. Lett. 77 (2000) 7.
[10] M. Peccianti, G. Assanto, Opt. Lett. 26 (2001) 1791.
[11] G. Assanto, M. Peccianti, K. Brzdakiewicz, A. De Luca, C. Umeton, J. Nonlin. Opt. Phys. Mater. 12 (2003) 123.
[12] D. Jović, M. Petrović, M. Belić, J. Schroeder, Ph. Jander, C. Denz, Opt. Exp. 13 (2005) 10717.